



Contents lists available at UGC-CARE

International Journal of Pharmaceutical Sciences and Drug Research

[ISSN: 0975-248X; CODEN (USA): IJPSPP]

Available online at www.ijpsronline.com

Research Article

Design, Synthesis, Molecular Docking, Antitubercular, Antimicrobial and Antioxidant Studies of Some Novel 3-(((1H-Benzo[d]imidazol-2-yl)methyl)thio)-5H-[1,2,4] Triazino[5,6-b]indole Derivatives

Sreelatha Kamera¹, Vishnu K. Sharma², Srivani M¹, Achaiah Garlapati^{1*}¹Department of Pharmaceutical Chemistry, University College of Pharmaceutical Sciences, Kakatiya University, Warangal, Telangana, India.²Department of Pharmacoinformatics, National Institute of Pharmaceutical Education and Research, Mohali, Punjab, India.

ARTICLE INFO

Article history:

Received: 16 June, 2023

Revised: 30 June, 2023

Accepted: 01 July, 2023

Published: 30 July, 2023

Keywords:

Benzimidazole, Indole, Antitubercular, Antibacterial, Antifungal, Antioxidant activity, Molecular docking, *Mycobacterium tuberculosis*, InhA.

DOI:

10.25004/IJPSDR.2023.150414

ABSTRACT

A series of novel 3-(((1H-benzo[d]imidazol-2-yl)methyl)thio)-5H-[1,2,4]triazino[5,6-b]indole derivatives (3a-3j) were synthesized by reacting different substituted 5H-[1,2,4]triazino[5,6-b]indole-3-thiols with substituted (2-chloromethyl)-1H-benzo(d)imidazoles in the presence of KOH and water in good yields. The structures of the newly synthesized compounds were confirmed by spectroscopic techniques such as ¹H-NMR, ¹³C-NMR, IR and mass spectrometry. The *in-vitro* antitubercular activity of the synthesized compounds was evaluated against *Mycobacterium tuberculosis* (Mtb) H37Rv (ATCC 27294) using MABA (Microplate Alamar Blue Assay) method. Compounds 3b, 3c, and 3i showed good antitubercular activity against Mtb with MIC value of $6.25 \pm 0.00 \mu\text{g/mL}$. Also, the *in-vitro* antimicrobial activities of the compounds were evaluated against various bacterial and fungal strains using the two-fold serial dilution technique and most of the compounds exhibited moderate activities with MIC values in the range of 63.33 ± 1.44 to $>500 \mu\text{g/mL}$ against the tested microorganisms. The compounds (3a-3j) were also tested for their *in-vitro* antioxidant activities by DPPH radical scavenging activity method and among the series, compounds 3e, 3a, and 3g exhibited strong antioxidant activity with IC_{50} values of 10.85 ± 0.05 , 12.18 ± 0.13 and $12.57 \pm 0.17 \mu\text{g/mL}$ respectively compared to the standard ascorbic acid (IC_{50} value, $5.85 \pm 0.04 \mu\text{g/mL}$). Further, molecular docking studies were performed to investigate the binding affinities as well as the interaction of these compounds with Mtb InhA target protein. *In-silico* ADME predictions showed that all the synthesized compounds have drug-like properties and exhibited good oral bioavailability.

INTRODUCTION

Despite its prehistoric origins, tuberculosis (TB) remains the deadliest infectious disease to afflict mankind,^[1,2] causing around 10.6 million new cases and 1.6 million deaths globally every year.^[3] TB is an airborne disease caused by the bacillus *Mycobacterium tuberculosis* (Mtb), which can spread by coughing or sneezing and usually attacks the lungs (Pulmonary TB) but can also invade other organs of the body such as the kidney, spine, and brain (Extrapulmonary TB). Primarily two types of TB-related conditions exist: Latent TB infection and active TB disease.^[4-7] About one-fourth of the world's population is estimated

to have latent TB infection, and about 5 to 10% of people infected with TB will eventually get symptoms and develop (Active) TB disease.^[3,8,9] Treatment of TB comprises a 6-month regimen of 'isoniazid-rifampicin-ethambutol-pyrazinamide,' all four drugs for the first two months, followed by isoniazid and rifampicin for the remaining 4 months.^[3,10] However, drug-resistant TB (DR-TB) such as rifampicin-resistant TB (RR-TB: Resistance to rifampicin) and multidrug-resistant TB (MDR-TB: Resistance to rifampicin and isoniazid) has emerged and continues to be a major public health threat.^[11] About 450 000 new cases of RR-TB were estimated by WHO in 2021.^[3] Both MDR-TB and RR-TB require treatment with second-line

*Corresponding Author: Dr. Achaiah Garlapati

Address: Department of Pharmaceutical Chemistry, University College of Pharmaceutical Sciences, Kakatiya University, Warangal, Telangana, India.

Email ✉: achaiah1960@gmail.com

Tel.: +91-8639329570

Relevant conflicts of interest/financial disclosures: The authors declare that the research was conducted in the absence of any commercial or financial relationships that could be construed as a potential conflict of interest.

Copyright © 2023 Sreelatha Kamera *et al.* This is an open access article distributed under the terms of the Creative Commons Attribution-NonCommercial-ShareAlike 4.0 International License which allows others to remix, tweak, and build upon the work non-commercially, as long as the author is credited and the new creations are licensed under the identical terms.

drugs such as aminoglycosides (streptomycin, kanamycin, amikacin), fluoroquinolones (ofloxacin, gatifloxacin, moxifloxacin, levofloxacin), ethionamide, prothionamide, para-aminosalicylic acid, cycloserine, etc., repurposed drug clofazimine and three new recently approved drugs bedaquiline, delamanid, and pretomanid that are often associated with more side effects, longer treatment times, and higher costs. In addition, MDR-TB strains that are resistant to second-line drugs have emerged, which further complicates the treatment leading to pre-extensively drug-resistant TB (pre-XDR-TB: resistant to rifampicin and any fluoroquinolone) and extensively drug-resistant TB (XDR-TB: resistance to rifampicin, any fluoroquinolone and at least one of bedaquiline or linezolid), which are even more challenging to treat and there is a low success rate of treatment for these conditions.^[3, 11-18] Therefore, there is an urgent need for the development of new anti-TB drugs with novel mechanisms of action to combat MDR/XDR TB.

Nitrogen-containing heterocycles are privileged scaffolds and possess remarkable biological activities and physicochemical properties. Approximately 75% of the FDA approved drugs contain a nitrogen heterocycle and this percentage is reportedly rising each year.^[19,20] Among the nitrogen-heterocyclic compounds, benzimidazoles and triazino[5,6-b]indole derivatives constitute a significant class of biologically relevant molecules due to their extensive spectrum of biological activities and clinical applications. Benzimidazole is found in several naturally occurring products like vitamin B 12, histidine, purines etc., and several clinically approved drugs contain benzimidazole such as telmisartan, candesartan (Angiotensin II receptor blockers), albendazole, mebendazole etc., (Anthelmintic drugs), esomeprazole, lansoprazole, etc., (Proton-pump inhibitors), droperidol, pimozide, etc., (Typical antipsychotic drugs) etc.^[21,22] Benzimidazole derivatives show significant antibacterial,^[23] antifungal,^[24] antitubercular^[25] activities apart from various other activities.^[26,27] On the other hand, a literature review of triazino[5,6-b] indole derivatives revealed that they were associated with antibacterial,^[28,29] antifungal,^[30] antitubercular,^[31] antioxidant,^[32] and several other biological activities.^[33-39] Taking into account of the biological significance of benzimidazole and triazino[5,6-b] indole derivatives, we have designed and synthesized a new series of 3-(((1H-benzo[d]imidazol-2-yl)methyl)thio)-5H-[1,2,4]triazino[5,6-b]indole derivatives (Fig. 1) which contain both the important pharmacophores in a single hybrid, as a part of our ongoing research to design and synthesize diverse heterocyclic scaffolds through pharmacophore hybridization approach in order to find novel and potent therapeutic agents.^[40-42] All the newly synthesized compounds were screened for their antitubercular, antimicrobial and antioxidant activities. *In-silico* investigations, including molecular docking and ADME predictions, have also been carried out and

discussed in order to obtain deeper understanding of the structure-activity relationship of the compounds under investigation.

MATERIALS AND METHODS

Chemicals

All reagents and solvents were purchased from commercial sources Sigma Aldrich, Bangalore, Spectrochem, Mumbai and Finar, Ahmedabad, India and were used without further purification. Melting points were determined MEL TEMP electrothermal melting point apparatus and are uncorrected. The progress of the reactions was monitored by thin-layer chromatography (TLC) using precoated silica gel 60 F254 plates, Merck, Germany, and the spots are observed using UV light as the visualizing agent or iodine vapors. The compounds were purified by column chromatography on silica gel 60–100 mesh (Merk) using ethyl acetate: hexane and chloro-form: methanol in different ratios as mobile phase. The IR spectra were recorded on a Perkin Elmer FTIR spectrometer in KBr pellets and the wave numbers are given in cm^{-1} . Both ^1H -NMR and ^{13}C -NMR spectra were recorded on a Bruker AVANCE 500 MHz spectrometer using DMSO- d_6 as solvent. Chemical shifts are reported in parts per million relative to tetramethyl silane ($\delta = 0$). Coupling constants are reported in hertz. Splitting patterns are defined by s (singlet), d (doublet), dd (double doublet), t (triplet) or m (multiplet). The electron spray ionization mass spectra (ESI-MS) were recorded on a time-of-flight mass spectrometer. The molecular docking studies were carried out by using Schrodinger software (Schrödinger, LLC, NY, USA).

Synthetic Procedure

The target compounds 3-(((1H-benzo[d]imidazol-2-yl)methyl)thio)-5H-[1,2,4]triazino[5,6-b]indole derivatives (3a-3j) were synthesized using the procedure illustrated in Fig. 2.

Step (i): General procedure for the synthesis of N-alkyl isatins

Initially, N-Alkylation of the appropriate isatins followed by cyclization to the corresponding 5H-[1,2,4]triazino[5,6-b]indol-3-thiols was carried out adopting previously reported methods.^[43,44] Briefly, substituted isatin (1 equiv) in DMF was reacted with appropriate alkyl halide (1.1 equiv) in the presence of K_2CO_3 (1.2 equiv) base and KI (0.2 equiv) catalyst and the reaction mixture was stirred at 80°C for 5 to 24 hours. TLC monitored the progress of the reaction and the reaction mixture was added to HCl (0.5 M, 50 mL) and extracted with ethyl acetate (50 mL). The ethyl acetate layer was washed with brine and dried over MgSO_4 . The crude product was purified by recrystallization using ethanol to yield corresponding N-alkyl isatins.

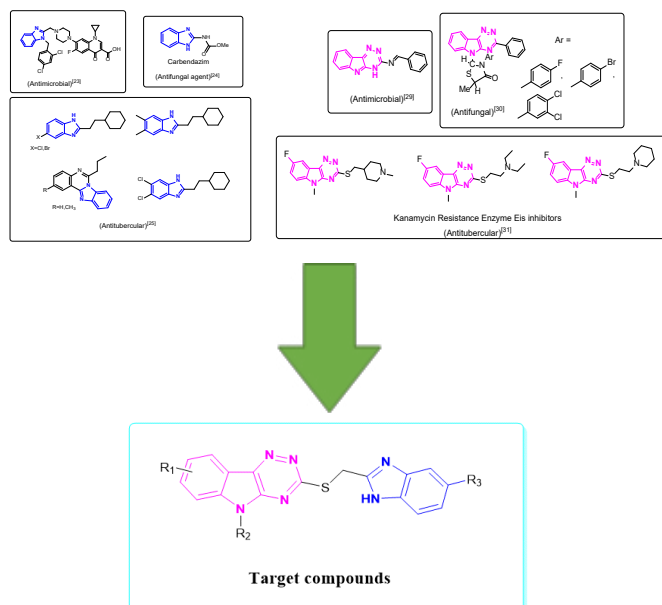


Fig. 1: Design strategy of 3-(((1H-benzo[d]imidazol-2-yl)methyl)thio)-5H-[1,2,4]triazino[5,6-b]indole derivatives.

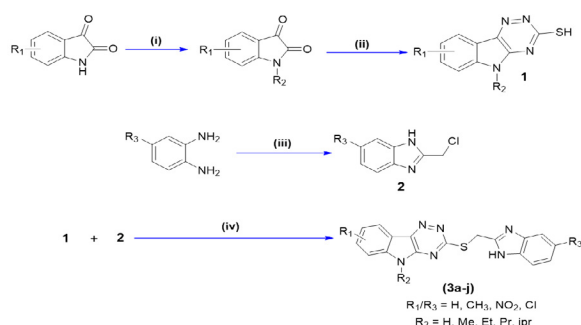


Fig. 2: General Synthetic Route for the Synthesis of 3-(((1H-benzo[d]imidazol-2-yl)methyl)thio)-5H-[1,2,4]triazino[5,6-b]indole derivatives (3a-3j)^a

^aReagents and conditions: (i) K_2CO_3 , DMF, alkyl halide, KI, 80°C, 5-24 h; (ii) Thiosemicarbazide, K_2CO_3 , H_2O , 100°C, reflux, 3-16 hours; (iii) chloroacetic acid, 4N HCl, reflux, 4 h; (iv) KOH, H_2O , 90°C, reflux, 24 hours.

Step (ii): General procedure for the synthesis of 5H-[1,2,4]triazino[5,6-b]indol-3-thiols (1)

To a stirred suspension of N-alkylated isatin (10 mmol) in aqueous K_2CO_3 (15 mmol in 50 mL of water) was added thiosemicarbazide (10 mmol) and the reaction mixture was refluxed for 3 to 16 hours. After cooling down to room temperature, the solution was acidified with glacial acetic acid and left overnight. The precipitate obtained was filtered and washed with a mixture of water/acetic acid (24:1 v/v) and the solid formed was triturated with hot DMF, filtered, and dried to yield compound 1.

Step (iii): General procedure for the synthesis of 2-chloromethyl-1H-benzimidazoles (2)

2-Chloromethyl-1H-benzimidazole derivatives were prepared based on previously reported methods.^[45,46]

A mixture of 4-substituted-O-phenylenediamine (1-mmol) in 4N HCl (10 mL) and chloroacetic acid (2 mmol) was refluxed for 4 hours and the reaction mixture was allowed to cool down and neutralized with ammonium hydroxide solution. The precipitate obtained was filtered, dried and recrystallized using methanol to yield compound 2.

Step (iv): General procedure for the synthesis of 3-(((1H-benzo[d]imidazol-2-yl)methyl)thio)-5H-[1,2,4]triazino[5,6-b]indole Derivatives (3a-3j)

The target compounds were synthesized by following the previously reported methods in literature.^[36,44,47] To a solution of 5H-[1,2,4]triazino[5,6-b]indol-3-thiol (1) (1 mmol), potassium hydroxide (65 mg, 1-mmol, 86.4%), and water (5 mL) stirred at room temperature for 2 hours, was added (2-(chloromethyl)-1H-benzo[d]imidazole) (2) and the resulting mixture was stirred at 90°C for 24 hours. TLC monitored the reaction's progress, and after the reaction was completed, the mixture was evaporated to obtain the crude product. Purification was done by column chromatography using mixture of ethyl acetate and hexane as mobile phase to yield the light yellow-colored final products (3a-3j). The physical properties of the final compounds are represented in Table 1. All the synthesized compounds were characterized by spectroscopic methods such as 1H -NMR, ^{13}C -NMR, Mass and IR.

Spectral Data of the Synthesized Derivatives (3a-3j)

3-(((1H-benzo[d]imidazol-2-yl)methyl)thio)-8-methyl-5H-[1,2,4]triazino[5,6-b]indole (3a)

IR (KBr, $\bar{\nu}$, cm^{-1}): 3469.05 (N-H), 3064.26 (C-H, Ar), 2979.08 (C-H aliphatic), 1606.69 (C=N), 1563.40 (C=C), 1373.85 (CH_3 bend); 1H -NMR (500 MHz, DMSO- d_6 , δ , ppm): 12.54 (s, NH indole), 12.18 (s, NH benzimidazole), 7.64 – 7.63 (m, 2H, ArH), 7.58 (dd, $J_1 = 7.5$ Hz, $J_2 = 6.4$ Hz, 1H, ArH), 7.41 (d, $J = 7.5$ Hz, 1H, ArH), 7.23 – 7.21 (m, 2H, ArH), 7.05 (t, $J = 7.9$ Hz, 1H, ArH), 4.42 (s, 2H, SCH_2), 2.38 (s, 3H, CH_3); ^{13}C -NMR (120 MHz; DMSO- d_6 , δ , ppm): 171.13, 145.06, 144.82, 139.99, 138.28, 138.19, 137.86, 131.91, 129.46, 122.16, 121.51, 119.73, 118.09, 118.08, 114.41, 113.54, 23.61, 21.20; Mass (ESI-MS, m/z): 347.41 $[M+H]^+$.

3-(((1H-benzo[d]imidazol-2-yl)methyl)thio)-9-nitro-5H-[1,2,4]triazino[5,6-b]indole (3b)

IR (KBr, $\bar{\nu}$, cm^{-1}): 3469.05 (N-H), 3127.23 (C-H, Ar), 2962.79 (C-H, aliphatic), 1667.53 (C=N), 1580.42 (C=C), 1345.25 (NO_2 stretch); 1H -NMR (500 MHz, DMSO- d_6 , δ , ppm): 12.54 (s, NH indole), 12.15 (s, NH benzimidazole), 7.96 (d, $J = 7.5$ Hz, 1H, ArH), 7.81 (d, $J = 7.5$ Hz, 1H, ArH), 7.71 (d, $J = 7.5$ Hz, 1H, ArH), 7.58 (d, $J = 7.5$ Hz, 1H, ArH), 7.47 (t, $J = 7.5$ Hz, 1H, ArH), 7.25 – 7.22 (m, 2H, ArH), 4.34 (s, 2H, SCH_2); ^{13}C -NMR (120 MHz; DMSO- d_6 , δ , ppm): 171.19, 144.82, 143.89, 142.02, 138.28, 138.19, 137.51, 136.60, 134.60, 122.16, 121.51, 118.09, 117.01, 115.07, 114.74, 114.41, 23.62; Mass (ESI-MS, m/z): 378.38 $[M+H]^+$.



3-(((1H-benzo[d]imidazol-2-yl)methyl)thio)-9-chloro-5H-[1,2,4]triazino[5,6-b]indole (3c)

IR (KBr, $\bar{\nu}$, cm^{-1}): 3459.06 (N-H), 3086.23 (C-H, Ar), 2955.06 (C-H, aliphatic), 1672.65 (C=N), 1582.01 (C=C), 754.24 (C-Cl); $^1\text{H-NMR}$ (500 MHz, DMSO- d_6 , δ , ppm): 12.52 (s, NH indole), 12.18 (s, NH benzimidazole), 7.63 (d, $J = 7.5$ Hz, 1H, ArH), 7.58 (d, $J = 7.5$ Hz, 1H, ArH), 7.36 (d, $J = 7.5$ Hz, 1H, ArH), 7.23 – 7.10 (m, 4H, ArH), 4.56 (s, 2H, SCH_2); $^{13}\text{C-NMR}$ (120 MHz; DMSO- d_6 , δ , ppm): 174.43, 144.82, 141.84, 141.71, 141.15, 138.28, 138.19, 130.34, 122.16, 121.51, 121.09, 120.72, 118.09, 115.85, 114.41, 113.01, 23.64; Mass (ESI-MS, m/z): 366.83 $[\text{M}]^+$, 368.83 $[\text{M}+2]^+$.

3-(((1H-benzo[d]imidazol-2-yl)methyl)thio)-5H-[1,2,4]triazino[5,6-b]indole (3d)

IR (KBr, $\bar{\nu}$, cm^{-1}): 3301.12 (N-H), 3058.26 (C-H, Ar), 2872.23 (C-H, aliphatic), 1646.21 (C=N), 1601.02 (C=C); $^1\text{H-NMR}$ (500 MHz, DMSO- d_6 , δ , ppm): 12.54 (s, NH indole), 12.15 (s, NH benzimidazole), 7.68 (d, $J = 7.5$ Hz, 1H, ArH), 7.63 (d, $J = 7.5$ Hz, 1H, ArH), 7.58 (d, $J = 7.5$ Hz, 1H, ArH), 7.49 (d, $J = 7.5$ Hz, 1H, ArH), 7.23 – 7.20 (m, 3H, ArH), 7.11 (t, $J = 7.6$ Hz, 1H, ArH), 4.45 (s, 2H, SCH_2); $^{13}\text{C-NMR}$ (120 MHz; DMSO- d_6 , δ , ppm): 171.31, 145.04, 144.82, 140.34, 139.44, 138.28, 138.19, 129.52, 122.16, 121.84, 121.51, 118.09, 117.78, 114.41, 113.75, 23.62; Mass (ESI-MS, m/z): 333.39 $[\text{M}+H]^+$.

3-(((1H-benzo[d]imidazol-2-yl)methyl)thio)-5-methyl-5H-[1,2,4]triazino[5,6-b]indole (3e)

IR (KBr, $\bar{\nu}$, cm^{-1}): 3421.05 (N-H), 3089.14 (C-H, Ar), 2865.52 (C-H, aliphatic), 1654.36 (C=N), 1565.02 (C=C), 1421.08 (CH_3 bend); $^1\text{H-NMR}$ (500 MHz, DMSO- d_6 , δ , ppm): 12.18 (s, NH benzimidazole), 7.62 – 7.60 (m, 2H, ArH), 7.49 (d, $J = 7.5$ Hz, 1H, ArH), 7.37 (d, $J = 7.5$ Hz, 1H, ArH), 7.26 – 7.19 (m, 4H, ArH), 4.44 (s, 2H, SCH_2), 3.89 (s, 3H, CH_3); $^{13}\text{C-NMR}$ (120 MHz; DMSO- d_6 , δ , ppm): 170.73, 148.95, 144.81, 144.79, 141.92, 138.28, 138.19, 131.68, 123.15, 122.86, 122.16, 121.51, 119.83, 118.09, 114.41, 29.66, 23.64; Mass (ESI-MS, m/z): 347.41 $[\text{M}+H]^+$.

3-(((1H-benzo[d]imidazol-2-yl)methyl)thio)-5-ethyl-5H-[1,2,4]triazino[5,6-b]indole (3f)

IR (KBr, $\bar{\nu}$, cm^{-1}): 3468.69 (N-H), 3135.02 (C-H, Ar), 2953.56 (C-H, aliphatic), 1664.10 (C=N), 1572.39 (C=C), 1465.05 (CH_2 bend); $^1\text{H-NMR}$ (500 MHz, DMSO- d_6 , δ , ppm): 12.16 (s, NH benzimidazole), 7.63 (d, $J = 7.5$ Hz, 1H, ArH), 7.58 (d, $J = 7.5$ Hz, 1H, ArH), 7.45 (d, $J = 7.5$ Hz, 1H, ArH), 7.36 (d, $J = 7.5$ Hz, 1H, ArH), 7.26 – 7.23 (m, 4H, ArH), 4.54 (s, 2H, SCH_2), 4.32 (q, $J = 7.2$ Hz, 2H, NCH_2), 1.37 (t, $J = 7.2$ Hz, 3H, NCH_2CH_3); $^{13}\text{C-NMR}$ (120 MHz; DMSO- d_6 , δ , ppm): 168.83, 149.99, 144.82, 143.79, 143.52, 138.28, 138.19, 130.89, 122.52, 122.28, 122.16, 121.51, 121.40, 40.82, 23.66, 13.33; Mass (ESI-MS, m/z): 361.44 $[\text{M}+H]^+$.

3-(((1H-benzo[d]imidazol-2-yl)methyl)thio)-5-propyl-5H-[1,2,4]triazino[5,6-b]indole (3g)

IR (KBr, $\bar{\nu}$, cm^{-1}): 3460.23 (N-H), 3128.04 (C-H, Ar), 2965.42 (C-H, aliphatic), 1672.58 (C=N), 1589.07 (C=C); $^1\text{H-NMR}$ (500 MHz, DMSO- d_6 , δ , ppm): 12.18 (s, NH benzimidazole),

7.63 (d, $J = 7.5$ Hz, 1H, ArH), 7.59 (d, $J = 7.5$ Hz, 1H, ArH), 7.44 (d, $J = 7.5$ Hz, 1H, ArH), 7.36 (d, $J = 7.5$ Hz, 1H, ArH), 7.26 – 7.21 (m, 4H, ArH), 4.52 (s, 2H, SCH_2), 4.09 (t, $J = 7.2$ Hz, 2H, NCH_2), 1.59 – 1.53 (m, 2H, NCH_2CH_2), 0.80 (t, $J = 7.2$ Hz, 3H, CH_3); $^{13}\text{C-NMR}$ (120 MHz; DMSO- d_6 , δ , ppm): 169.53, 148.74, 144.82, 143.40, 143.22, 138.28, 138.19, 131.43, 122.64, 122.49, 122.16, 121.51, 121.11, 118.09, 114.41, 108.22, 48.27, 23.61, 21.12, 11.98; Mass (ESI-MS, m/z): 375.47 $[\text{M}+H]^+$.

3-(((1H-benzo[d]imidazol-2-yl)methyl)thio)-5-isopropyl-5H-[1,2,4]triazino[5,6-b]indole (3h)

IR (KBr, $\bar{\nu}$, cm^{-1}): 3469.02 (N-H), 3134.65 (C-H, Ar), 2914.02 (C-H, aliphatic), 1673.05 (C=N), 1596.02 (C=C); $^1\text{H-NMR}$ (500 MHz, DMSO- d_6 , δ , ppm): 12.20 (s, NH benzimidazole), 7.73 (d, $J = 7.5$ Hz, 1H, ArH), 7.58 (d, $J = 7.5$ Hz, 1H, ArH), 7.46 (d, $J = 7.5$ Hz, 1H, ArH), 7.39 (d, $J = 7.5$ Hz, 1H, ArH), 7.27 – 7.22 (m, 4H, ArH), 5.08 – 5.05 (m, 1H, NCH), 4.54 (s, 2H, SCH_2), 1.61 (d, 6H, CH_3); $^{13}\text{C-NMR}$ (120 MHz; DMSO- d_6 , δ , ppm): 169.86, 150.78, 144.82, 143.82, 140.22, 138.28, 138.19, 133.25, 122.99, 122.16, 122.15, 121.51, 120.50, 118.09, 114.41, 49.51, 23.63, 19.74; Mass (ESI-MS, m/z): 375.47 $[\text{M}+H]^+$.

3-(((5¹-nitro-1H-benzo[d]imidazol-2-yl)methyl)thio)-5H-[1,2,4]triazino[5,6-b]indole (1-8i)

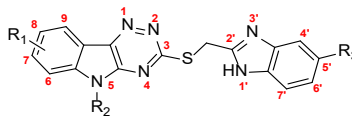
IR (KBr, $\bar{\nu}$, cm^{-1}): 3450.13 (N-H), 3175.07 (C-H, Ar), 2954.34 (C-H, aliphatic), 1683.34 (C=N), 1598.01 (C=C), 1347.89 (NO_2 stretch); $^1\text{H-NMR}$ (500 MHz, DMSO- d_6 , δ , ppm): 12.54 (s, NH indole), 12.18 (s, NH benzimidazole), 8.39 (d, $J = 7.5$ Hz, 1H, ArH), 7.92 (d, $J = 7.5$ Hz, 1H, ArH), 7.85 (d, $J = 7.5$ Hz, 1H, ArH), 7.67 (d, $J = 7.5$ Hz, 1H, ArH), 7.43 (d, $J = 7.5$ Hz, 1H, ArH), 7.16 (t, $J = 7.6$ Hz, 1H, ArH), 7.01 (t, $J = 7.5$ Hz, 1H, ArH), 4.44 (s, 2H, SCH_2); $^{13}\text{C-NMR}$ (120 MHz; DMSO- d_6 , δ , ppm): 169.86, 150.78, 144.82, 143.82, 140.22, 138.28, 138.19, 133.25, 122.99, 122.16, 122.15, 121.51, 120.50, 118.09, 114.41, 49.51, 23.62, 19.74; Mass (ESI-MS, m/z): 378.38 $[\text{M}+H]^+$.

3-(((5¹-methyl-1H-benzo[d]imidazol-2-yl)methyl)thio)-5H-[1,2,4]triazino[5,6-b]indole (3j)

IR (KBr, $\bar{\nu}$, cm^{-1}): 3459.17 (N-H), 3143.09 (C-H, Ar), 2974.52 (C-H, aliphatic), 1645.98 (C=N), 1587.03 (C=C); $^1\text{H-NMR}$ (500 MHz, DMSO- d_6 , δ , ppm): 12.54 (s, NH indole), 12.16 (s, NH benzimidazole), 7.68 (d, $J = 7.5$ Hz, 1H, ArH), 7.59 (d, $J = 7.5$ Hz, 1H, ArH), 7.54 (s, 1H, ArH), 7.45 (d, $J = 7.5$ Hz, 1H, ArH), 7.20 (t, $J = 7.6$ Hz, 1H, ArH), 7.11 – 7.10 (m, 2H, ArH), 4.47 (s, 2H, SCH_2), 2.34 (s, 3H, CH_3); $^{13}\text{C-NMR}$ (120 MHz; DMSO- d_6 , δ , ppm): 171.31, 145.73, 145.04, 140.34, 139.44, 137.59, 135.48, 130.93, 129.52, 123.89, 121.84, 118.08, 117.78, 117.30, 113.80, 113.76, 23.65, 21.20; Mass (ESI-MS, m/z): 347.41 $[\text{M}+H]^+$.

Biological Evaluation**Antitubercular activity**

The antitubercular activity of all the synthesized compounds (3a-3j) was tested against *M. tuberculosis*

Table 1: Physical properties of the synthesized compounds (3a-3j)

Compound code	R ₁	R ₂	R ₃	Molecular Formula	Molecular Weight	Melting Point [°C]	R _f [*] value	Yield [%]
3a	8-CH ₃	H	H	C ₁₈ H ₁₄ N ₆ S	346.41	253–255	0.52	65
3b	9-NO ₂	H	H	C ₁₇ H ₁₁ N ₇ O ₂ S	377.38	283–285	0.58	55
3c	9-Cl	H	H	C ₁₇ H ₁₁ ClN ₆ S	366.83	265–268	0.47	58
3d	H	H	H	C ₁₇ H ₁₂ N ₆ S	332.39	290–293	0.44	82
3e	H	Methyl	H	C ₁₈ H ₁₄ N ₆ S	346.41	230–232	0.45	60
3f	H	ethyl	H	C ₁₉ H ₁₆ N ₆ S	360.44	281–283	0.41	53
3g	H	Propyl	H	C ₂₀ H ₁₈ N ₆ S	374.47	262–264	0.34	65
3h	H	Isopropyl	H	C ₂₀ H ₁₈ N ₆ S	374.47	272–274	0.46	58
3i	H	H	5'- NO ₂	C ₁₇ H ₁₁ N ₇ O ₂ S	377.38	282–284	0.58	60
3j	H	H	5'- CH ₃	C ₁₈ H ₁₄ N ₆ S	346.41	283–285	0.53	62

*(Chloroform/Ethyl acetate) 9:1

(Vaccine strain, H37RV: ATCC No-27294) using the microplate alamar blue assay (MABA) method.^[48,49] This methodology shows good correlation with proportional and BACTEC radiometric methods and is non-toxic. It utilizes a thermally stable reagent alamar blue, and briefly, the stock solutions of the tested compounds were prepared in dimethyl sulfoxide. 96 well plates were treated with 100 µL of the Middlebrook 7H9 broth and serial dilution of the test compounds were made directly on plate. The final concentrations of the test compounds were 100 to 0.2 µg/mL. Isoniazid, rifampicin and pyrazinamide were used as standard drugs. 200 µL of sterile deionized water was added to all outer perimeter wells of sterile 96 well plates to minimize the medium's evaporation in the test wells during incubation. These plates were covered and sealed with parafilm and were incubated at 37°C for five days. After this time, 25 µL of freshly prepared mixture of Almar blue reagent and 10% tween 80 in 1:1 ratio was added to the plate and incubated for a further 24 hours. A blue color in the well indicates no bacterial growth, while a pink color indicates as growth. The MIC was defined as the lowest drug concentration, which prevented the color change from blue to pink and MIC values were expressed in µg/mL.

Antibacterial and antifungal activity

The title compounds 3-(((1H-benzo[d]imidazol-2-yl)methyl)thio)-5H-[1,2,4]triazino[5,6-b]indole derivatives (3a-3j) were screened for their *in-vitro* antibacterial and antifungal activity using tube dilution method.^[50] Gram-positive bacteria: *Bacillus subtilis* (MTCC 441), *Staphylococcus aureus* (ATCC 25923), gram-negative bacteria: *Escherichia coli* (ATCC 25922), *Klebsiella pneumonia* (ATCC 700603) and fungal strains: *Aspergillus niger* (MTCC 404), *Saccharomyces cerevisiae* (MTCC 1344)

were the test organisms used in the present study. The inhibition by the synthesized compounds was compared with the standard drugs ampicillin and miconazole for antibacterial and antifungal activity, respectively. The stock solutions of standard drugs and test compounds were prepared in DMSO having 1-mg/mL concentration. Further dilutions of the compounds and standard drugs in the test medium were prepared in 1 to 1000 µg/mL concentrations. Testing was carried out in Mueller–Hinton broth medium for the antibacterial assay and sabouraud dextrose broth medium for antifungal assay at pH 7.4. Minimum inhibitory concentrations (MIC) were determined using the twofold serial dilution technique.^[50] A control test was performed containing inoculated broth supplemented with only DMSO. The samples were incubated at 37 ± 1°C for 24 hours (for bacterial species), at 37 ± 1°C for 24 hours (*S. cerevisiae*) and at 37 ± 1°C for 48 hours (*A. niger*), respectively. Antimicrobial screening results were recorded in terms of the lowest concentration of test substances that inhibited the growth of microorganisms i.e., MIC expressed in µg/mL and were represented in Table 2.

Antioxidant activity

The synthesized compounds' *in-vitro* antioxidant activity was evaluated spectrophotometrically using 1,1-diphenyl-2-picrylhydrazyl (DPPH) radical scavenging assay.^[51,52] DPPH is a stable free radical with a deep purple color that shows maximum absorbance at 517 nm. DPPH assay provides an easy and rapid way to evaluate antioxidant activities in a relatively short time, hence it can be useful to assess various products at a time. The stock solutions of the test compounds were prepared in DMSO to achieve the concentration of 1-mg/mL and then dilutions were made to obtain concentrations of 5, 10, 15, 25, and 50 µg/mL.



A DPPH (0.1 mM) solution in methanol (1.0 mL) was added to 3 mL of different test sample concentrations and allowed to stand at room temperature in a dark chamber for 30 minutes. The change in color from deep violet to light yellow was measured at 517 nm using a spectrophotometer. Methanol was used as a blank solvent and a fresh DPPH solution in methanol served as the control. The experiment was carried out in triplicate and the average values are taken as final result. The ability of the title compounds at tested concentration to scavenge DPPH radicals were calculated using the following equation.

$$\% \text{ of DPPH radical scavenging activity} = [(A - B)/A] \times 100$$

where, A is the absorbance of the control and B is the absorbance of the test sample. Ascorbic acid was used as a standard. The antioxidant activity for all the compounds was expressed as IC_{50} i.e., the concentration of the samples that causes 50% scavenging of DPPH radical in $\mu\text{g/mL}$. IC_{50} was calculated from equation of line obtained by plotting a graph of concentration versus %inhibition. The lower IC_{50} value indicates high antioxidant capacity.

Molecular Docking Protocol

The three-dimensional (3D) X-ray crystal structure of Mtb enoyl acyl carrier protein reductase (InhA) in complex with (3S)-1-cyclohexyl-N-(3,5-dichlorophenyl)-5-oxopyrrolidine-3-carboxamide (PDB ID: 4TZK; resolution: 1.62Å) was accessed from RCSB Protein Data Bank (<http://www.rcsb.org>).^[53] Molecular docking simulations were carried out to identify the best binding orientation and molecular interactions of the synthesized compounds (3a-3j) with the target protein using Glide SP docking module of Schrödinger software.^[54,55] Before docking, 'protein preparation wizard' module of Schrödinger Software^[56-58] was used to prepare and optimize the crystal structure by removing water molecules, heteroatoms and addition of hydrogens, missing atoms, bonds, and charges etc., followed by protein structure minimization using 'Optimized Potentials for Liquid Simulations-2005' (OPLS-2005) force field.^[59] Ligand preparation and optimization was performed by using 'LigPrep' module of Schrödinger Software^[60] which generates energy minimized 3D structures of the studied compounds and co-crystallized ligand. The 'receptor grid generation' module of Schrödinger software was used to generate the active site for docking of the ligands by considering the centroid of the co-crystallized ligand with a grid box size of 10x10x10 Å. The validation of molecular docking was done by re-docking the co-crystallized ligand into the active site of the target protein and comparing the resulting poses and root mean square deviation (RMSD) value between the docked ligand and co-crystallized ligand. The glide score, glide energy and hydrogen bonding interactions, pi-pi stacking interactions,

and pi-cation stacking interactions of all the synthesized compounds (3a-3j) were presented in Table 3.

In-silico ADME Studies

One of the most important aspects of drug discovery and development is the prediction of absorption, distribution, metabolism and excretion (ADME) parameters prior to experimental studies in order to avoid late-stage failures of drug candidates.^[61] In the present study, QikProp module of Schrödinger software^[62] was used for the prediction of ADME properties of all the synthesized compounds (3a-3j). Molecular descriptors such as #stars, MW, PSA, HBD, HBA, QPlogPo/w, QPlogS, QPPCaco, %HOA, Rule of 5, #rtvFG, CNS, QPlogBB, QPPMDCK, QPlogKhsa and #metab were calculated using Qikprop and were represented in Table 4.

RESULTS AND DISCUSSION

Chemistry

The synthesis of the designed compounds 3-(((1H-benzo[d]imidazol-2-yl)methyl)thio)-5H-[1,2,4]triazino[5,6-b]indole derivatives (3a-3j) was carried out as depicted in Fig. 2. N-alkylation of 8/9-substituted isatins was obtained with commercially available alkyl halides in the presence of K_2CO_3 , KI in N, N-dimethylformamide (DMF) and were cyclized to the corresponding 5H-1,2,4-triazino-[5,6-b]indole-3-thiols (1) in the presence of aqueous K_2CO_3 and thiosemicarbazide at reflux condition. The second intermediate: 2-chloromethyl-1H-benzo(d)imidazole (2) was prepared by refluxing of 4-substituted-O-phenylenediamine in 4N HCl and chloroacetic acid. Finally, nucleophilic substitution to displace the chloride of the 5-substituted 2-chloromethyl-1 H-benzo(d)imidazole (2) with thiol (1) was achieved by refluxing in KOH and water at ambient temperature and target compounds (3a-3j) were obtained in good yields (53–82%). The structures of synthesized compounds were confirmed on the basis of their $^1\text{H-NMR}$, $^{13}\text{C-NMR}$, ESI-MASS and FTIR spectral analysis. The presence of singlet signal in $^1\text{H-NMR}$ spectra in the range of 12.52 to 12.54 ppm indicates the presence of NH proton of triazino[5,6-b]indole in compounds 3a-3d, 3i, and 3j in addition to the appearance of singlet signal from δ 12.15 to 12.20 ppm, due to the presence of NH proton of benzimidazole moiety. The singlet signal for two protons in the range of δ 4.42 to 4.52 ppm indicates the presence of methylene group (-S-CH₂) in all the synthesized compounds. Singlet signal integrated for three protons at δ 2.38, δ 2.34 and δ 3.89 ppm indicates the presence of methyl group in compounds 3a, 3j and 3e, respectively. All the aromatic and heteroaromatic protons appeared in the range of δ 7.01 to 8.39 ppm. The $^{13}\text{C-NMR}$ spectra of all compounds showed signals in the range of δ 169–174 ppm due to the presence of carbon atom attached to sulfur (-C-S- group). Signals between δ 144 to 150 ppm are assigned to sp² carbon of benzimidazole (-N=C-NH-)

and a singlet signal observed in the range of δ 23.61–23.66 ppm is assignable to the methylene carbon ($-S-CH_2-$). The mass spectra ESI-MS results were in accordance with the theoretical m/z . The IR spectra of compounds showed characteristic absorption bands between 3300 to 3469 cm^{-1} due to $-NH$ stretching and aromatic (C-H) stretching bands appeared between 3058 to 3175 cm^{-1} . The appearance of absorption band at 754 cm^{-1} in compound 3c indicates the presence of C-Cl group. Detailed spectral data of target compounds 3a-3j was mentioned in the experimental section.

Biological Activities

Antitubercular activity

All the synthesized compounds 3a-3j were evaluated for their *in-vitro* antimycobacterial activity against Mtb H37Rv (ATCC 27294) using MABA method.^[48,49] Isoniazid, rifampicin and pyrazinamide were used as reference drugs. The results were expressed as MIC values and presented in Table 2. The *in-vitro* assay results indicate that all the synthesized derivatives exhibited mild to moderate activity against Mtb with MIC values in the range of 6.25 ± 0.00 - >50 $\mu g/mL$. Compounds 3b, and 3c having electron withdrawing groups 9-nitro and 9-chloro substitution on triazino[5,6-b]indole moiety and compound 3i with 5-nitro group on benzimidazole moiety exhibited the highest growth inhibitory effect against Mtb H37Rv with MIC values of 6.25 ± 0.00 $\mu g/mL$ compared to the MIC value of 3.125 ± 0.00 $\mu g/mL$ shown by the standard drug pyrazinamide. Compounds 3f and 3g were found to be moderately potent with MIC values of 12.5 ± 0.00 $\mu g/mL$. Compounds 3e and 3h exhibited mild inhibitory effect with MIC value of 25 ± 0.00 $\mu g/mL$ and compounds 3a and 3j showed no activity (MIC > 50 $\mu g/mL$).

Antibacterial and antifungal activity

The *in-vitro* antimicrobial activity of synthesized compounds was evaluated against two gram positive bacteria (*B. subtilis* (MTCC 441), *S. aureus* (ATCC 25923)), two gram negative bacteria (*E. coli* (ATCC 25922), *K. pneumonia* (ATCC 700603)) and two fungal strains: *A. niger* (MTCC 404), *S. cerevisiae* (MTCC 1344) using two-fold serial dilution technique.^[50] Ampicillin and Miconazole were used as reference standards for antibacterial and antifungal activity. The results (Table 2) indicated that all compounds showed low antimicrobial activity against tested bacterial and fungal strains with MIC values in the range of 63.33 ± 1.44 - > 500 $\mu g/mL$ when compared to the standard drugs (Ampicillin, MIC value: 2.67 ± 1.15 $\mu g/mL$, Miconazole, MIC value: 4.67 ± 1.15 $\mu g/mL$). Among the series, compound 3c having 9-chloro substitution on triazino[5,6-b]indole moiety exhibited mild antibacterial activity against *S. aureus*, *E. coli* with MIC value of 63.33 ± 1.44 $\mu g/mL$ and antifungal activity against *A. niger* with MIC value of 125 ± 0.00 $\mu g/mL$. Compound 3d also

exhibited mild antibacterial activity against *S. aureus*, *B. subtilis* and *K. pneumonia* with MIC value of 64.5 ± 3.46 , 64 ± 2.60 and 63.33 ± 1.44 $\mu g/mL$, respectively and exhibited mild antifungal activity against *A. niger* with MIC value of 125.67 ± 1.15 $\mu g/mL$. Compounds 3g and 3j exhibited mild antifungal activity against *A. niger* with MIC values of 126.33 ± 2.31 and 125 ± 0.00 $\mu g/mL$ and compound 3e exhibited mild antifungal activity against *S. cerevisiae* with MIC value of 125.66 ± 1.15 . Compounds 3f and 3i showed good activity against *E. coli* with MIC values of 62.5 ± 0.00 and 63.33 ± 1.44 $\mu g/mL$, respectively.

Antioxidant activity

The antioxidant activity of synthesized compounds was assessed by employing DPPH free radical scavenging assay method^[51,52] using ascorbic acid as standard reference compound. The results indicate that all the compounds 3a-3j showed mild to moderate antioxidant activity with IC_{50} values in the range of 10.85 to 23.45 $\mu g/mL$ compared to the standard ascorbic acid (IC_{50} value: 5.85 $\mu g/mL$). Among the series, compound 3e exhibited the most potent *in-vitro* DPPH activity with IC_{50} value of 10.85 $\mu g/mL$ and compounds 3a and 3g exhibited significant potency with IC_{50} values of 12.18 and 12.57 $\mu g/mL$ respectively.

Molecular Docking Studies

Molecular docking is a valuable *in-silico* drug discovery and development tool that can predict the binding affinity between molecules and biological targets.^[63,64] Enoyl-acyl carrier protein reductase enzyme InhA, is necessary for Mtb survival because it is involved in the biosynthesis of mycolic acids, one of the main components of Mtb cell wall. It is the front-line antitubercular drug isoniazid's main target and does not have a human equivalent. Isoniazid is a prodrug and the mycobacterial catalase-peroxidase enzyme KatG converts it into the reactive isonicotinyl acyl radical, which can subsequently form a covalent adduct with the nicotinamide adenine dinucleotide cofactor of InhA (Isoniazid-NAD adduct) that actually inhibits InhA.^[65-67] Mutations in the prodrug-activating enzyme KatG contribute to a high percentage of isoniazid resistance,^[68] so direct inhibitors of InhA that do not require KatG activation would be promising candidates.^[69] Hence in the present study, molecular docking of all the synthesized compounds (3a-3j) was performed against the active site of Mtb InhA enzyme structure (PDB code: 4TZK) using Glide docking program (Glide, Schrödinger, LLC, New York, NY, 2020).^[54,55] This crystal structure was chosen because of its good resolution (1.62Å) and InhA is bound to (3S)-1-cyclohexyl-N-(3,5-dichlorophenyl)-5-oxopyrrolidine-3-carboxamide, the most potent inhibitor with IC_{50} value of 0.39 μM . To evaluate the effectiveness of the Glide docking protocol, co-crystal inhibitor was extracted from the crystal structure of InhA (PDB: 4TZK) obtained from the protein data bank and redocked into the active site of Mtb InhA. This produced a binding



Table 2: *In-vitro* antibacterial, antifungal, antitubercular and antioxidant activities of synthesized compounds (3a-3j)

Compound code	Minimum inhibitory concentration (µg/mL)										DPPH activity IC ₅₀ value ^c , µg/mL
	Antibacterial activity ^a					Antifungal activity ^a			Antitubercular activity ^b <i>M. tuberculosis H37Rv</i> (ATCC 27294)		
	<i>S. aureus</i> (ATCC 25923)	<i>B. subtilis</i> (MTCC 441)	<i>E. coli</i> (ATCC 25922)	<i>K. pneumonia</i> (ATCC 700603)	<i>A. niger</i> (MTCC 404)	<i>S. cerevisiae</i> (MTCC 1344)					
3a	250 ± 0.00	125.67 ± 1.15	>500	62.5 ± 0.00	>500	500 ± 0.00	>50			12.18 ± 0.13	
3b	125.67 ± 1.15	63.33 ± 1.44	251.33 ± 2.31	500 ± 0.00	>500	-	6.25 ± 0.00			14.24 ± 0.22	
3c	63.33 ± 1.44	126.33 ± 2.31	64.17 ± 2.89	251.33 ± 2.31	125 ± 0.00	-	6.25 ± 0.00			22.34 ± 0.06	
3d	64.5 ± 3.46	64 ± 2.60	>500	63.33 ± 1.44	125.67 ± 1.15	-	50 ± 0.00			14.98 ± 0.40	
3e	126 ± 1.73	252 ± 3.46	250 ± 0.00	125 ± 0.00	251.33 ± 2.31	125.66 ± 1.15	25 ± 0.00			10.85 ± 0.05	
3f	250.67 ± 1.15	250.67 ± 1.15	62.5 ± 0.00	252 ± 3.46	-	500 ± 0.00	12.5 ± 0.00			15.85 ± 0.12	
3g	251.33 ± 2.30	250 ± 0.00	252 ± 3.46	500 ± 0.00	126.33 ± 2.31	500 ± 0.00	12.5 ± 0.00			12.57 ± 0.17	
3h	125 ± 0.00	500 ± 0.00	500 ± 0.00	>500	252 ± 3.46	500 ± 0.00	25 ± 0.00			22.13 ± 0.31	
3i	250.67 ± 1.15	251.33 ± 2.30	63.33 ± 1.44	250 ± 0.00	-	500 ± 0.00	6.25 ± 0.00			23.45 ± 0.11	
3j	250 ± 0.00	250 ± 0.00	250.67 ± 1.15	500 ± 0.00	125 ± 0.00	250 ± 0.00	>50			14.22 ± 0.51	
Ampicillin	2.67 ± 1.15	2.67 ± 1.15	2.67 ± 1.15	2.67 ± 1.15	-	-	-			-	
Miconazole	-	-	-	-	4.67 ± 1.15	4.67 ± 1.15	-			-	
DMSO (-ve Control)	NA	NA	NA	NA	NA	NA	-			-	
Broth Control	NG	NG	NG	NG	NG	NG	-			-	
Isoniazid	-	-	-	-	-	-	1.6 ± 0.00			-	
Rifampicin	-	-	-	-	-	-	1.6 ± 0.00			-	
Pyrazinamide	-	-	-	-	-	-	3.125 ± 0.00			-	
Ascorbic acid	-	-	-	-	-	-	-			5.85 ± 0.04	

NA - No Activity; NG - No Growth

^{a,c} Data are mean \pm standard deviation of three individual determinations. (-): Not detected.^b Data are mean \pm standard deviation of two individual determinations by MABA visual

conformation that was identical to that found in the ligand's native crystal structure, with a root mean square deviation (RMSD) of 0.18 Å, confirming the docking procedure's accuracy and reliability. All the synthesized molecules showed good binding energies and glide docking scores ranging from -57.80 to -44.12 kcal/mol and -9.17 to -8.58 kcal/mol, respectively. All compounds (3a-3k) showed H-bonding interaction with the amino acid Tyr158, which is considered to be the crucial interaction for catalytic mechanism of InhA. The amino acid residues Leu 207, Ile 215, Ala 211, Ile202, Met 199, Ala 198, Pro 193, Met 161, Tyr 158, Ala 157, Pro 156, Met 155, Phe 149, Met 103, Phe 97 and Met 98 have been found to be involved in hydrophobic interactions that are essential for inhibiting the enoyl ACP reductase enzyme. It was observed that the synthesized compounds' *in-vitro* antitubercular activities do not agree with the glide gscores. The most active compounds 3b, 3i exhibited glide gscores of -8.98 and -8.60 kcal/mol respectively and exhibited H-bonding interaction between the N atom at second position of triazino[5,6-b]indole moiety with the amino acid Tyr158 and a π - π stacking between the imidazole ring of benzimidazole moiety and Phe 149. Compound 3c exhibited glide gscore of -8.76 kcal/mol and showed H-bonding interaction with the amino acid Tyr 158. N-propyl/ethyl substituted triazino[5,6-b]indole compounds 3g and 3f with mild activity, exhibited higher glide gscores of -9.17 Kcal/mol and showed H-bonding interaction with the amino acid Tyr158 and π - π stacking interaction with Tyr 158 and/or Phe 149. Compound 3h with mild activity also exhibited higher glide gscore of -9.15 K cal/mol and showed H-bonding interactions with Tyr158 and Gly 96 and a π - π stacking interaction with Phe 149 amino acid. The glide gscore, glide energy, glide emodel energy, hydrogen bonding and π - π interaction of all the synthesized compounds (3a-3j) and co-crystal ligand are reported in Table 3 and the 2D interactions of the ligands with the active site residues of Mtb InhA were presented in Fig. 3.

***In-silico* ADME Analysis**

Further, we have performed the absorption, distribution, metabolism and excretion (ADME) prediction studies for all the synthesized compounds 3a-3j using QikProp module of Schrodinger software.^[62] Qikprop predicts #stars parameter based on the number of properties or descriptors that fall outside the 95% range of similar values for known drugs. It represents the overall ADME-compliance score and the predicted #stars value for all the compounds was found to be in the range of 0-1 (the acceptable range is 0-5), suggesting that all the molecules are more drug-like. Various physicochemical properties like: molecular weight (MW), polar surface area (PSA), number of donor hydrogen bonds (HBD), number of acceptor hydrogen bonds (HBA), predicted octanol/water partition coefficient (QPlogPo/w), predicted

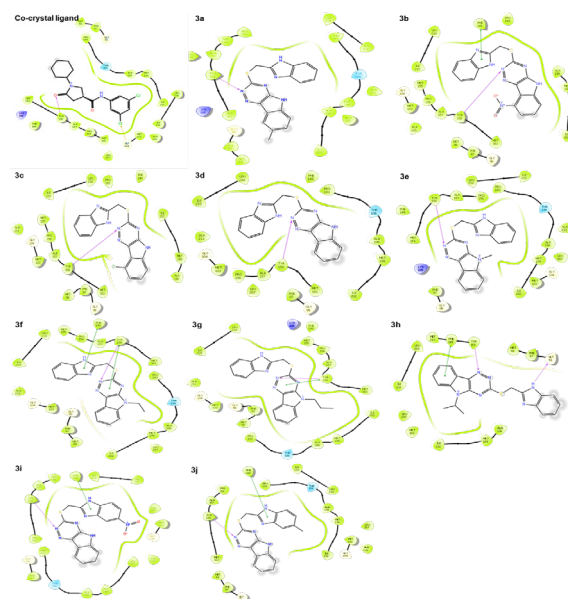


Fig. 3: 2D Molecular docking interactions of the co-crystal ligand and synthesized compounds 3a-3j into the active site of *M. tuberculosis* InhA protein (PDB: 4TZK) (pink color lines indicate hydrogen bonds, green lines indicate π - π stacking interactions).

aqueous solubility (QPlogS), predicted apparent CaCo-2 cell permeability in nm/sec (QPPCaco), predicted percent human oral absorption scale (%HOA), number of violations of Lipinski's rule of five (Rule of 5), number of reactive functional groups (#rtvFG), predicted central nervous system activity (CNS), predicted brain/blood partition coefficient (QPlogBB), predicted apparent MDCK cell permeability in nm/sec (QPPMDCK), prediction of binding to human serum albumin (QPlogKhsa) and number of likely metabolic reactions (#metab) have been studied for all the compounds and are presented in Table 4.

The Qikprop predicted number of violations of Lipinski's rule of five were found to be 0 for all the compounds and obeyed the drug-likeness rule of five, such as MW < 500, QPlogPo/w < 5, HBD ≤ 5, HBA ≤ 10.^[70,71] This suggests the drug-likeness behavior of all the molecules and oral bioavailability could be accounted. The predicted aqueous solubility (QPlogS) values ranged from -5.1 to -6.48 and predicted polar surface area (PSA) values ranged from 64.32-123.7 and are found to be within the acceptable ranges. The predicted apparent CaCo-2 cell permeability in nm/sec (QPPCaco) was found to be between 75.83-1668.22 (acceptable range: <25 poor, >500 great), which suggests that all the compounds have excellent intestinal absorption capabilities. It was found that all the synthesized compounds displayed %human oral absorption (%HOA) values ranging from 76.04 to 100% (acceptable range: >80% high, <25% poor) which suggests good oral absorption of the compounds. The number of reactive functional groups (#rtvFG) for all compounds were predicted to be 0 (acceptable range: 0-2). The predicted central nervous system activity (CNS) was



Table 3: Molecular docking results of the synthesized compounds (3a-3j)

Compound code	Docking Interactions					
	Glide gscore (Kcal/mol)	Glide emodel (Kcal/mol)	Glide energy (Kcal/mol)	Hydrogen bonding (Distance in Å)	$\pi - \pi$ stacking	Halogen bond
Co-crystal ligand	-10.58	-98.01	-59.52	Tyr 158 (2.05)	-	Gly 104
3a	-8.63	-82.19	-53.89	Tyr 158 (2.76)	-	-
3b	-8.98	-84.81	-55.14	Tyr158 (2.66)	Phe 149	-
3c	-8.76	-82.94	-54.734	Tyr 158 (2.63)	-	-
3d	-8.58	-80.52	-52.98	Tyr 158 (2.43)	-	-
3e	-9.0	-82.76	-54.62	Tyr 158 (2.41)	-	-
3f	-9.17	-79.06	-51.23	Tyr 158 (2.63)	Tyr 158, Phe 149	-
3g	-9.17	-69.54	-44.12	Tyr 158 (2.32)	Tyr 158	-
3h	-9.15	-76.77	-50.81	Tyr 158 (2.76), Gly 96 (1.89)	Phe 149	-
3i	-8.60	-85.60	-57.85	Tyr 158 (2.67)	Phe 149	-
3j	-8.84	-84.16	-55.15	Tyr 158 (2.61)	Phe 149	-

Table 4: Predicted ADME properties of synthesized compounds (3a-3j) using Qikprop^[62]

Compound code	3a	3b	3c	3d	3e	3f	3g	3h	3i	3j	Acceptable range
#stars ^a	0	1	0	0	0	0	0	0	0	0	0-5
MW ^b	346.41	377.38	366.83	332.38	346.41	360.44	374.46	374.46	377.38	346.41	130.0-725.0
PSA ^c	79.63	121.4	78.53	79.65	66.87	64.42	64.32	66.49	123.71	79.59	7.0-200.0
HBD ^d	2	2	2	2	1	1	1	1	2	2	0.0-6.0
HBA ^e	4.5	5.5	4.5	4.5	4.5	4.5	4.5	4.5	5.5	4.5	2.0-20.0
QPlogPo/w ^f	3.51	2.75	3.77	3.21	4.1	4.48	4.86	4.72	2.634	3.5	-2.0-6.5
QPlogS ^g	-5.72	-5.25	-5.72	-5.1	-5.78	-6.05	-6.46	-6.48	-5.37	-5.68	-6.5-0.5
QPPCaco ^h	606.69	114.32	704.99	605.96	1339.08	1664.04	1668.22	1382.38	75.83	608.78	<25 poor, >500 great
% HOA ⁱ	100	79.86	100	95.51	100	100	100	100	76.04	100	>80% high, <25% poor
Rule of 5 ^j	0	0	0	0	0	0	0	0	0	0	maximum is 4
#rtvFG ^k	0	0	0	0	0	0	0	0	0	0	0-2
CNS ^l	-1	-2	0	-1	0	0	0	0	-2	-1	-2 to +2
QPlogBB ^m	-0.87	-1.71	-0.63	-0.84	-0.48	-0.46	-0.54	-0.55	-1.93	-0.86	-3.0-1.2
QPPMDCK ⁿ	426.64	70	1079.31	426	1004.54	1252.57	1257.14	1043.87	45.57	432.39	<25 poor, >500 great
QPlogKhsa ^o	0.48	0.28	0.42	0.33	0.54	0.64	0.75	0.77	0.29	0.47	-1.5-1.5
#metab ^p	2	2	1	1	1	1	1	1	2	2	1-8

^aoverall ADME-compliance score; ^bMolecular weight in Da; ^cPolar surface area; ^dEstimated number of donor hydrogen bonds; ^eEstimated number of acceptor hydrogen bonds; ^fPredicted octanol/water partition coefficient; ^gPredicted aqueous solubility; ^hPredicted apparent CaCo-2 cell permeability in nm/sec; ⁱPredicted human oral absorption on 0 to 100% scale; ^jNumber of violations of Lipinski's rule of five; ^kNumber of reactive functional groups; ^lPredicted central nervous system activity; ^mPredicted brain/blood partition coefficient; ⁿPredicted apparent MDCK cell permeability in nm/sec; ^oPrediction of binding to human serum albumin; ^pNumber of likely metabolic reactions; ^qPredicted IC₅₀ value for blockage of HERG K⁺ channels.

found be in the range of -2 to 0 (acceptable range: -2 to +2), predicted brain/blood partition coefficient (QPlogBB) ranged from -1.93 to -0.46 (acceptable range: -3.0-1.2), predicted apparent MDCK cell permeability in nm/sec

(QPPMDCK) ranged from 45.57-1257.57 (acceptable range: <25 poor, >500 great) suggesting that all the compounds are CNS inactive and do not cross blood-brain barrier. It was observed that the predicted QPlogKhsa values are